論文 / 著書情報
Article / Book Information

Title	Structure and optical properties of ZnO/Mg_0.2_Zn_0.8_O superlattices
Authors	A. Ohtomo,M. Kawasaki,I. Ohkubo,H. Koinuma,T. Yasuda,Y. Segawa
Citation	Applied Physics Letters, Vol. 75, No. 7,
Pub. date	1999, 7
URL	http://scitation.aip.org/content/aip/journal/apl
Copyright	Copyright (c) 1999 American Institute of Physics

Structure and optical properties of $ZnO/Mg_{0.2}Zn_{0.8}O$ superlattices

A. Ohtomo[a] and M. Kawasaki
Department of Innovative and Engineered Materials, Tokyo Institute of Technology, Yokohama 226-8502, Japan

I. Ohkubo and H. Koinuma[b]
Materials and Structures Laboratory, Tokyo Institute of Technology, Yokohama 226-8503, Japan

T. Yasuda[c] and Y. Segawa
Photodynamic Research Center, The Institute of Physical and Chemical Research, Sendai 980-0868, Japan

(Received 27 April 1999; accepted for publication 23 June 1999)

$ZnO/Mg_{0.2}Zn_{0.8}O$ superlattices with a band-gap offset of about 0.5 eV were epitaxially grown by laser molecular-beam epitaxy on a sapphire(0001) substrate using a ZnO buffer layer. The superlattice structure with a period ranging from 8 to 18 nm was clearly verified by cross-sectional transmission electron microscopy, Auger depth profile, and x-ray diffraction. As the well layer thickness decreased below 5 nm, the photoluminescence peak and absorption edge in the photoluminescence excitation spectra showed a blueshift, indicating a quantum-size effect. © *1999 American Institute of Physics.* [S0003-6951(99)04033-4]

Recently, considerable attention is being paid to ZnO as a wide-gap oxide semiconductor. ZnO has a band gap of 3.34 eV at room temperature, thus it is a potential candidate for ultraviolet light emission. We have demonstrated room-temperature laser action with a low threshold ($24\,kW/cm^2$) from optically pumped ZnO thin films composed of hexagonally shaped nanocrystals closely assembled in a honeycomb fashion.[1] There are three interesting findings concerning this phenomenon. First, the stimulated emission process was caused by exciton–exciton collision even at room temperature because of the very large exciton binding energy (60 meV).[2] Second, the threshold of this excitonic process was very low when the nanocrystalline size was tuned at about 50 nm (Ref. 3). Third, the longitudinal cavity was automatically formed by making use of the grain boundaries between hexagonal nanocrystals acting as mirrors.[4,5] Recently, we have reported that $Mg_xZn_{1-x}O$ alloy films can be prepared by pulsed-laser deposition, which show a higher band gap up to 4 eV at $x=0.33$ and have similar lattice constants.[6] The emission process with exciton recombination further can be enhanced if such low-dimensional structures as quantum wells, wires, and dots are constructed.

Here, we report the structural characterization and optical properties of $ZnO/Mg_{0.2}Zn_{0.8}O$ superlattices. A quantum-confinement effect was observed in photoluminescence (PL) and photoluminescence excitation (PLE) spectroscopies.

$ZnO/Mg_xZn_{1-x}O$ superlattices were fabricated by laser molecular-beam epitaxy (MBE), i.e., pulsed-laser deposition from ceramic targets along with reflection high-energy electron diffraction (RHEED) observation in an ultra-high-vacuum chamber.[7] The Mg content of the barrier layer was chosen at $x=0.20$, corresponding to a band offset of about 0.5 eV at the heterointerface with pure ZnO. The oxygen pressure was kept constant at 1×10^{-6} Torr during the deposition. Before deposition of the superlattice, a 100-nm-thick ZnO buffer layer was grown on a sapphire(0001) substrate at 550 °C. Then, a superlattice with ten periods was fabricated on the ZnO buffer layer at 650 °C. The ZnO layer thickness (L_W) was varied from 1.7 to 12 nm, maintaining the $Mg_{0.2}Zn_{0.8}O$ layer thickness (L_B) constant at 6.2 nm. A schematic of the superlattice structure is given in Fig. 1(a). The layer thickness was controlled by the deposition time by taking into account the deposition rate predetermined by the single-layer deposition experiments. In order to determine the Mg content of the barrier layer, $Mg_xZn_{1-x}O$ single-layer films were grown on sapphire under the same condition using a $Mg_{0.1}Zn_{0.9}O$ target and the composition was analyzed by inductively coupled plasma (ICP) optical emission spectroscopy by dissolving the films in HNO_3 (0.1 mol/l) solution. Note that we have chosen $x=0.1$ of the target because of Mg condensation during growth due to the larger vapor pressure of ZnO than that of MgO.[6]

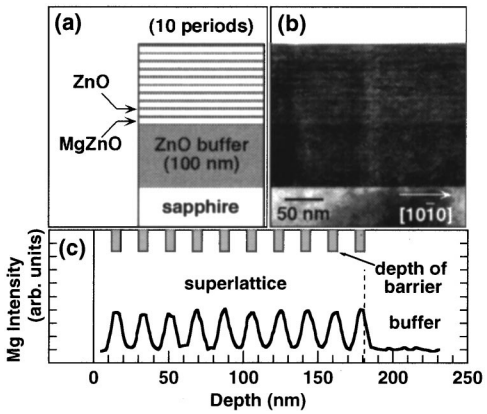

FIG. 1. Cross-sectional schematic (a) and TEM image (b) of a $ZnO/Mg_{0.2}Zn_{0.8}O$ superlattice with $L_W=5.7$ nm and $L_B=6.2$ nm. The depth profile of the Mg signal intensity in AES was measured for a superlattice with $L_W=12$ nm and $L_B=6.2$ nm (c).

[a]Electronic mail: ohtomo@oxide.rlem.titech.ac.jp
[b]Also a member of CREST, Japan Science and Technology Corporation.
[c]Present address: Department of Electronic Materials School of Science and Engineering, Ishinomaki Senshu University, 1 Shinmito, Minamisakai Ishinomaki 986-8580, Japan.

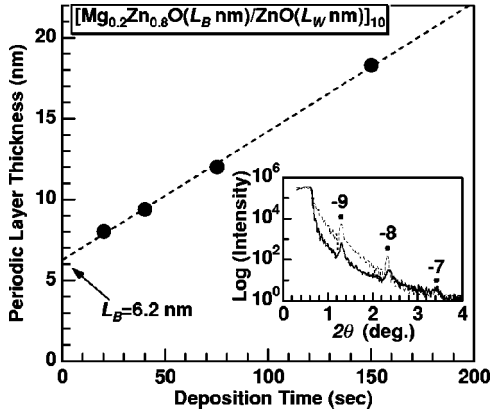

FIG. 2. The period of superlattices estimated from the XRD patterns is plotted as a function of deposition time for the well layer thickness. The barrier thickness was constant at 6.2 nm, while the well layer thickness was varied from 1.7 to 12 nm. The inset shows a typical x-ray diffraction pattern measured for a superlattice with $L_W = 1.7$ nm (solid line) and simulated curve (dotted line).

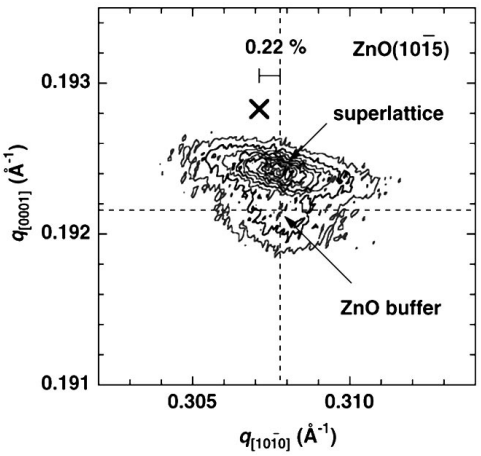

FIG. 3. X-ray diffraction reciprocal space contour map around $(10\bar{1}5)$ diffraction for a superlattice sample with $L_W = 12$ nm. The buffer ZnO layer and superlattice have an identical $q[10\bar{1}0]$ value, indicating the barrier $Mg_{0.2}Zn_{0.8}O$ layer is strained to form a pseudomorphic epitaxial structure. The cross in the figure is the peak position for a thick $Mg_{0.2}Zn_{0.8}O$ film. The lattice mismatch is as small as 0.22%.

The surface morphology of the films was examined by a contact-mode atomic force microscope (AFM). The superlattice structure was characterized by cross-sectional transmission electron microscope (TEM), depth profiling using Auger electron spectroscopy (AES), and x-ray diffractometer (Philips, X'-pert MRD). The optical properties were characterized by PL using a continuous He–Cd laser beam (325 nm) and PLE using monochromatic light from a Xe lamp.

A fine streaky RHEED pattern was observed throughout the deposition. The surface morphology observed by AFM was similar to that for ZnO films reported previously.[8] The root-mean-square (rms) roughness of the superlattice was less than 1 nm over 2 μm$\times$2 μm area. Hexagonally shaped grains are closely packed. On the grains, atomically flat terraces and steps (0.5 nm high), aligned as hexagonal spirals, can be seen. When the superlattice was deposited directly on sapphire, the surface was quite rough (the rms roughness was about 10 nm). The insertion of the ZnO buffer layer was essential to grow smooth superlattice films. Moreover, the deposition temperatures for the ZnO buffer layer and for the superlattice were independently optimized to get a smooth surface.

Figure 1(b) shows the TEM image of a superlattice with $L_W = 5.7$ nm. The designed layer structure is clearly seen as a modulation of the contrast. The depth profile of the Mg content in the superlattice was measured by AES and plotted in Fig. 1(c). As can be clearly seen, regular oscillation was observed until the end of the superlattice, indicating that the interface diffusion at the bottom interfaces during the successive film deposition is negligible. X-ray reflection at a small incident angle was measured for all of the samples. A typical example is shown in the inset of Fig. 2. The solid line is obtained from the experiment and the dotted curve is a simulation, calculated by using a theoretical model[9] assuming the interface rms roughness of 1 nm as evaluated by the AFM image. Peaks corresponding to the superlattice reflection were consistently observed for all superlattices. The period deduced from the superlattice peaks is plotted in Fig. 2 as a function of the deposition time for the well layers. As can be seen, the periodic structure is in excellent agreement with the designed one.

In the superlattices composed of alloy semiconductors, the in-plane lattice mismatch is an important parameter in the case of strained superlattices. With increasing Mg content (x in $Mg_xZn_{1-x}O$) the a-axis length expands as $3.250 + 0.036x$.[6] Therefore, an in-plane lattice mismatch of 0.22% can be expected for the superlattice prepared in this study. This lattice constant change is much smaller than those for $3.189 - 0.077x$ in $Al_xGa_{1-x}N$ (Ref. 10) and $3.189 + 0.36x$ in $Ga_{1-x}In_xN$.[11] When the superlattice is under strain, the piezoelectric field proportional to the product of the strain and piezoelectric constant is induced. If the well layers are strained, electrons and holes confined in the well layers will be spatially separated due to the internal electric field. In the case of $ZnO/Mg_xZn_{1-x}O$ superlattices, the in-plane lattice mismatch is small enough to neglect the internal electric field. Even if there is an internal field, the choice of the ZnO buffer layer will produce an unstrained well ZnO layer and a strained $Mg_xZn_{1-x}O$ barrier layer.

Figure 3 shows a reciprocal space contour mapping for a superlattice with $L_W = 12$ nm around an asymmetric $(10\bar{1}5)$ plane of ZnO. Two peaks corresponding to the buffer layer and superlattice were observed. As can be seen, the superlattice and buffer ZnO have an identical $q[10\bar{1}0]$ value within experimental accuracy. The peak position measured for a thick $Mg_{0.2}Zn_{0.8}O$ layer is marked by a cross as well to show 0.22% mismatch in the plane. Therefore, in these superlattices, only the barrier layers are strained to form a pseudomorphic epitaxial structure.

Figure 4 shows PL and PLE spectra taken at 4.2 K for the superlattices with $L_W = 1.7$ and 3.1 nm. The PL peak shifts towards the higher-energy side as L_W decreases. When $L_W = 5.2$ nm, no detectable shift was observed. The two peaks in the PLE spectra indicated by open and filled triangles are assigned to the $n = 1$ quantum subband level and barrier layer absorption level, respectively. The positions of the latter peaks shown by filled triangles agree with the absorption edge for a 200-nm-thick $Mg_{0.2}Zn_{0.8}O$ film, indicat-

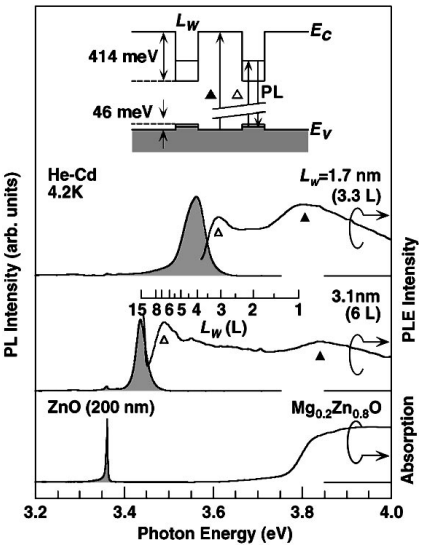

FIG. 4. PL and PLE spectra measured at 4.2 K for two of the superlattices ($L_W = 1.7$ and 3.2 nm). For comparison, the PL spectrum of a 50-nm-thick ZnO film and the absorption spectrum of a 200-nm-thick $Mg_{0.2}Zn_{0.8}O$ film are also shown. The ruler in the figure shows the calculated quantum subband energy as a function of well layer thickness [multiples of unit-cell height; $L_W/0.52$(L)].

ing that the carriers excited at the barrier layers are relaxed into the well layers and emit light upon recombination. In order to evaluate the relationship between the well layer thickness and the observed PLE peak position for the $n=1$ subband level, we have made a preliminary simulation by using the reported effective masses of electrons ($m_e^* = 0.28$) and holes ($m_h^* = 1.8$) and considering the finite-potential barrier. Since the discontinuities at the conduction and valence bands (ΔE_c and ΔE_v) have never been measured, we used the ratio of $\Delta E_c/\Delta E_v$ as a fitting parameter and obtained the best fit when $\Delta E_c/\Delta E_v = 9$, that is, $\Delta E_c = 414$ meV and $\Delta E_v = 46$ meV. The estimated $n=1$ quantum subband level for various well layer thicknesses is given as a ruler in Fig. 4.

The PL peaks show considerable broadening and Stokes shift by about 50 meV. The former is presumably due to the fluctuation of the well layer thickness. As reported earlier,[8] the ZnO film surface has spirally shaped steps with a unit-cell height (0.52 nm), therefore, these superlattices should have a well layer thickness fluctuation of ± 0.52 nm at minimum. The thickness fluctuations deduced from the full width at half maximum of the PL peaks, however, are larger than in the minimum case. The possible explanations for the peak broadening and Stokes shift could be (1) Mg content fluctuation in the barrier layers, (2) a bound state related to unintentionally doped impurities or crystallographic defects, and (3) a strain-induced band-gap modification of the barrier layers. The Mg content of $x=0.2$ is far above the solubility limit ($x=0.04$) (Ref. 12) of the bulk solid solution and close to the solubility limit of metastable thin films ($x=0.33$).[6] Therefore, we suspect reason (1) to be the most probable. Our preliminary results for superlattices using $x=0.10$ barrier layers showed higher-crystalline quality, better interface sharpness, and sharper PL peaks with a negligibly small Stokes shift.[13] Therefore, the uniformity of Mg content in the barrier layers significantly affects the optical properties of the ZnO/$Mg_xZn_{1-x}O$ superlattice.

In summary, we have shown that superlattices composed of oxide wide-gap semiconductors, ZnO and $Mg_{0.2}Zn_{0.8}O$ were successfully grown by employing a ZnO buffer layer. The PL and PLE spectra clearly showed a quantum-size effect. The Mg concentration of $x=0.2$ is close to the limit to obtain clear electronic structures at the heterointerfaces, probably due to the spatial fluctuation of Mg content in the barrier layer.

This work was partly supported by the JSPS Research for the Future Program in the area of Atomic-Scale Surface and Interface Dynamics (RFTF96P00205). One of the authors (A.O.) is supported by a JSPS Research Fellowship for Young Scientists. The authors thank Dr. Imai of the Asahi Chemical Industry Co., Ltd., for the AES measurement and Dr. T. Yaguchi and Dr. T. Kamino of Hitachi Instruments Eng., Co., Ltd., for the TEM observation.

[1] Y. Segawa, A. Ohtomo, M. Kawasaki, H. Koinuma, Z. K. Tang, P. Yu, and G. K. L. Wong, Phys. Status Solidi B **202**, 669 (1997).
[2] Z. K. Tang, P. Yu, G. K. L. Wong, M. Kawasaki, A. Ohtomo, H. Koinuma, and Y. Segawa, Solid State Commun. **103**, 459 (1997).
[3] A. Ohtomo, M. Kawasaki, Y. Sakurai, I. Ohkubo, R. Shiroki, Y. Yoshida, T. Yasuda, Y. Segawa, and H. Koinuma, Mater. Sci. Eng., B **54**, 24 (1998).
[4] Z. K. Tang, G. K. L. Wong, P. Yu, M. Kawasaki, A. Ohtomo, H. Koinuma, and Y. Segawa, Appl. Phys. Lett. **72**, 3270 (1998).
[5] P. Yu, Z. K. Tang, G. K. L. Wong, M. Kawasaki, A. Ohtomo, H. Koinuma, and Y. Segawa, J. Cryst. Growth **184/185**, 601 (1998).
[6] A. Ohtomo, M. Kawasaki, T. Koida, K. Masubuchi, H. Koinuma, Y. Sakurai, Y. Yoshida, T. Yasuda, and Y. Segawa, Appl. Phys. Lett. **72**, 2466 (1998).
[7] H. Koinuma, M. Kawasaki, and M. Yoshimoto, Mater. Res. Soc. Symp. Proc. **474**, 303 (1997).
[8] A. Ohtomo, Y. Sakurai, Y. Yoshida, P. Yu, Z. K. Tang, Ge. K. L. Wong, M. Kawasaki, H. Koinuma, and Y. Segawa, Mater. Eng., B **56**, 263 (1998).
[9] The simulations were carried out using a commercially available software (Win-Gixa, Philips) based on theoretical models in the literature, for example, L. G. Parratt, Phys. Rev. **95**, 359 (1954); D. K. G. de Boer, Phys. Rev. B **44**, 498 (1991).
[10] O. Ambacher, J. Smart, J. R. Shealy, N. G. Weimann, K. Chu, M. Murphy, W. J. Schaff, L. F. Eastman, R. Dimitrov, L. Wittmer, M. Stutzmann, W. Rieger and J. Hilsenbech, J. Appl. Phys. **85**, 3222 (1999).
[11] L. T. Romano, B. S. Krusor, M. D. McCluskey, D. P. Bour, and K. Nauka, Appl. Phys. Lett. **73**, 1757 (1998).
[12] J. F. Sarver, F. L. Katnack, and F. A. Hummel, J. Electrochem. Soc. **106**, 960 (1959).
[13] Y. Segawa, T. Yasuda, A. Ohtomo, and M. Kawasaki (unpublished).